Carbohydrate Polymers 101 (2014) 1033–1042

Contents lists available at ScienceDirect

Carbohydrate Polymers

journal homepage: www.elsevier.com/locate/carbpol

A carboxy methyl tamarind polysaccharide matrix for adhesion and growth of osteoclast-precursor cells

Sridhar Sanyasi[a], Ashutosh Kumar[b], Chandan Goswami[b], Abhijit Bandyopadhyay[c,*], Luna Goswami[a,**]

[a] School of Biotechnology, KIIT University, Patia, Bhubaneswar 751024, India
[b] School of Biological Sciences, National Institute of Science Education and Research, Institute of Physics Campus, Sachivalaya Marg, Bhubaneswar 751005, India
[c] Department of Polymer Science and Technology, University of Calcutta, 92, A.P.C. Road, Calcutta 700009, India

ARTICLE INFO

Article history:
Received 4 July 2013
Received in revised form 8 October 2013
Accepted 11 October 2013
Available online 27 October 2013

Keywords:
Polysaccharide
Hydrogels
Cell adhesion

ABSTRACT

Remodeling of bone by tissue engineering is a realistic option for treating several bone-related pathophysiological ailments such as osteoporosis, bone tumor, bone cancer or abnormal bone development. But, these possibilities are hindered due to lack of proper natural and biodegradable surface on which bone precursor cells can adhere efficiently and grow further. Here we describe the synthesis and characterization of a new hydrogel as an effective surface which can acts as a material for bone tissue engineering. This hydrogel has been prepared by chemically grafting a semi-synthetic polymer with a synthetic monomer, namely hydroxyethyl methacrylate (HEMA). Carboxy methyl tamarind (CMT) was selected as the semi-synthetic polymer. The hydrogel was prepared at different mole ratios and at the ratio of 1:10 (CMT:HEMA) yielded the best hydrogel as characterized by several physico-chemical analysis such as UV spectroscopy, FT-IR spectroscopy and swelling properties. We further demonstrate that this material is suitable for effective adhesion, growth and further clustering of bone precursor cells (RAW 264.7). This material is also compatible for growing other sensitive cells such as neuronal cells (Neuro2a) and human umbilical vein endothelial cells (HUVEC) demonstrating that this surface does not possess any cytotoxicity and is compatible for primary human cells too. We conclude that the hydrogel made of CMT:HEMA at a ratio of 1:10 can be suitable for bone tissue engineering and thus may have clinical as well as commercial application in future.

1. Introduction

Due to increment in average life span, prevalence in life style related disorders, cancer, indiscriminate use of chemotherapeutics and other pathophysiological problems, increasing bone disorders become a new clinical problem (Nauth et al., 2011). Partial or full repair and/or replacement of injured and/or defective bone are hoped to address these increasing cases of orthopedic problems. Recently significant development has been made in organ replacement as well as surgical reconstruction and use of artificial prostheses in order to treat the lost or defective organ or tissue has been reported (Thein-Han & Misra, 2009; Venkatesan, Ryu, Sudha, & Kim, 2012). In the context of bone tissue engineering, two procedures namely autograft and allograft are considered as ideal procedures for bone grafting. In the first procedure, bone is harvested from another part of the body and is used to fill the gap or used to graft the damaged bone which provides optimal osteoinductive, osteoconductive and osteogenic properties (Venkatesan et al., 2012). In second technique, namely allograft, osteoinductive and osteoconductive properties can be provided by cadaver bones (Venkatesan et al., 2012). However, both grafting procedures have few disadvantages (side effects). For example, in autograft procedures, complications are mainly related to wound healing, additional surgery, donor pain and an inadequate supply of bone to fill the gap (Venkatesan et al., 2012). Similarly, allograft leads to problems such as unwanted immunological responses. Allograft also bears the risk of acquiring transmissible diseases such as AIDS and hepatitis by tissues and fluids (Giannoudis, Dinopoulos, & Tsiridis 2005; Langer & Vacanti, 1993). In addition, changes in individual genotype, immune response and MHC complexes prevent use of bone from other sources for effective grafting (Reikeras, Shegarfi, Naper, Reinholt, & Rolstad, 2008; Reikeras, Sigurdsen, & Shegarfi, 2010; Shegarfi & Reikeras, 2009). Due to limited supply of natural bone that can be used for grafting, the need for

* Corresponding author. Tel.: +91 9433186957.
** Corresponding author. Tel.: +91 674 2725732.
E-mail addresses: abhijitbandyopadhyay@yahoo.co.in, abpoly@caluniv.ac.in (A. Bandyopadhyay), lbh_1975@yahoo.co.in (L. Goswami).

0144-8617/$ – see front matter © 2013 Elsevier Ltd. All rights reserved.
http://dx.doi.org/10.1016/j.carbpol.2013.10.047

synthetic bone substitutes which possess same physiochemical and biological properties as natural bone is ever increasing. These requirements enforce an increased attention to prepare artificial materials with similar biophysical properties (but without adverse immunological as well as other harmful biological effects) as bone graft substitutes or exenterate (Venkatesan et al., 2012).

Combinations of specific cell-type and specific scaffold-based tissue engineering have been considered as an alternative and better procedure for bone tissue engineering and repair. In past few decades, several techniques and materials have been employed for the orthopedic treatment (Venkatesan et al., 2012). For example, surfaces made of expensive and/or heavy metals such as titanium, zirconia, ferritic stainless steel, etc. were reported for bone tissue engineering which may exert heavy metal toxicity and other related problems over a long exposure (Hefti, Frischherz, Spencer, Hall, & Schlottig, 2010; Malheiro, Spear, Brooks, & Markaki, 2011). Often the cell adhesion and further growth on these surfaces are not up to the mark. For example, the number of osteoblasts successfully grow on titanium implant materials is less than 50% when compared to number of cells growing on fibronectin surface (Krause, Cowles, & Gronowicz, 2000). So far hydroxyapatite and/or gelatin based nanocomposites were also extensively tried as scaffold for bone tissue repair without much desired success (Azami et al., 2012). Though polymers are attractive materials for tissue engineering, their chemical properties, especially high hydrophobicity offer no control on cell adhesion or function because these surfaces are often reactive to many serum proteins and other hydrophobic biomolecules (Lieb et al., 2003). Often the proteins involved in cell adhesion are incompatible due to unwanted conformational changes on these hydrophobic surfaces. In addition, the surface stiffness of these materials affects the effective cell adhesion (Khatiwala, Peyton, & Putnam, 2006; Shih, Tseng, Lai, Lin, & Lee, 2011; Yang et al., 2011). All these factors enforce a continuous quest for alternative and economic materials for effective bone tissue engineering.

Among many scaffold materials made of diverse compounds such as hydroxyapatite, gelatin, collagen, chitosan, alginate and several nanocomposites, hydrogels offer many advantages, mainly due to their unique biocompatibility, flexible methods of synthesis, range of constituents, and desirable physical characteristics (Zambuzzi, Ferreira, Granjeiro, & Aoyama, 2011; Zhang et al., 2009). In addition, hydrogel-based bone tissue engineering is desirable as hydrogels have been recognized as “the material of choice” for many other applications such as drug delivery and regenerative medicine (Seliktar, 2012). Hydrogels can also be used as medium for controlled drug and protein delivery to different tissues and cultures. In general, the hydrogels are non-toxic, easy to use, cytocompatible, injectable and can be designed as bio-degradable (Glaesemann, 2011). Due to these properties, hydrogels represent synthetic biomaterials which are ideal for tissue engineering and tissue repair. These materials can serve as scaffolds that provide structural integrity to tissue constructs and serve as adhesives or barriers between tissue and material surfaces (Slaughter, Khurshid, Fisher, Khademhosseini, & Peppas, 2009). In spite of these huge potentialities, so far only few materials have fulfilled these requirements and new materials with better bio-compatibility and with no or limited side effects are required. For example, a glycosyl-nucleosyl-fluorinated (GNF) system has been recently reported to be compatible for stem cells and suitable for cell differentiation to osteoblasts. However, this material too has limitation as cells do not grow well on this surface (Ziane et al., 2011).

The present study mainly focuses to synthesize novel hydrogel with different hydrophobicity which should have no/less cytotoxicity and better biocompatibility. In this work we synthesized a new hydrogel from natural polysaccharides, namely from 2-HEMA and CMT as the starting materials. We further characterized different properties of these materials and optimized the ratio for the best physico-chemical properties. We also explored its biocompatibility by using different cells. We report that this new material is biocompatible with osteoclast-precursor cells as well as other sensitive cells such as neuronal cells (Neuro2a) and human umbilical vein endothelial cells (HUVEC) suggesting that this synthetic material can be used as a scaffold hydrogel for potential application in bone tissue engineering.

2. Materials and methods

2.1. Materials

Carboxy methyl tamarind (CMT) was kindly supplied by Hindustan Gums and Chemicals Limited, India. 2-Hydroxyethyl methacrylate (HEMA) (specific gravity = 1.069–1.075) was purchased from S.D. Fine Chemicals (Mumbai, India) and distilled twice before using it. Benzoyl peroxide was purchased from S.D. Fine Chemicals (Mumbai, India) and was used without further purification. Acetone was purchased from S.D. Fine Chemicals (Mumbai, India).

2.2. Preparation of CMT–HEMA grafted hydrogel

About 3 g of carboxy methyl tamarind (CMT) powder was dissolved in 100 ml of water and stirred in a magnetic stirrer for 2 h with 320 rpm to make a 3% (w/v) homogeneous solution. For grafting CMT and HEMA in 1:1 mole ratio, 20 ml of 3% (w/v) gelatinous CMT solution was added to 0.48 ml HEMA. A solution of benzoyl peroxide (0.1% of HEMA by wt) with HEMA was first prepared and quickly the solution so prepared was added to CMT solution. The reaction mixture was then purged with nitrogen to provide an inert atmosphere and allowed to stir at 320 rpm for 3 h at 75 °C. The reaction mixture was cooled and grafted hydrogel was separated from solvent, unreacted HEMA, initior and homopolymer of monomer (2-HEMA) by washing with acetone. The sample was dried at 50 °C in hot air oven for 24 h. The same method was performed for different mole ratio of CMT and HEMA (1: 0.5, 1:1, 1:5, 1:10, 1:20, 1:30, 1:50). The extent of grafting was determined from absorbance value derived from FTIR spectra of different hydrogels.

2.3. Swelling study

The swelling study of CMT–HEMA grafted copolymers were carried out in water under ambient temperature (approx. 25 °C). For swelling study a fixed weight of dry hydrogel sample was taken and immersed in water at pH 7. The sample was taken out at regular intervals of 5 s and wrapped with tissue paper to remove the residual water at the surface. The weight of the water soaked material was measured as the swelled weight. This procedure was continued till the hydrogel attains its maximum swelling weight after which no further increase in weight of the hydrogel was observed. The equilibrium swelling index (α) was calculated from the following equation where *wf* and *wi* are the final and the initial sample weights respectively.

$$\alpha = \left(\frac{wf - wi}{wi}\right) \times 100$$

2.4. Spectroscopic characterization

Spectroscopic characterization of hydrogel was done through Fourier transform infrared (FTIR) spectrophotometer (JASCO FTIR) within the spectral range of 400–4000 cm^{-1} and resolution 4 cm^{-1}. The FTIR spectra were recorded by tablet made of KBr powder on KBr plate. The UV–visible spectra taken for hydrogels of different

CMT:HEMA ratios are in the wave length range of 200–500 nm (Perkin Elmer Lamda 25, 1.27).

2.5. Biocompatibility

To test the biocompatibility, 2.5 μl hydrogel was spotted on the glass cover slips. The hydrogel was allowed to settle on the cover slips, air dried and subsequently used for the cell growth. Human macrophage cells, namely RAW264.7 cells were maintained in the DMEM media (Himedia, Bangalore) supplemented with 10% fetal bovine serum (Himedia, Bangalore) and penicillin (100 units/ml)–streptomycin (100 μg/ml) solution (Himedia, Bangalore) at 37 °C incubator with 5% CO_2. Similarly, Neuro2a cells were grown in DMEM media (Himedia, Bangalore) supplemented with 10% FBS (Himedia, Bangalore), penicillin (100 units per ml), streptomycin (100 micro gram per ml) and 2% L-glutamin (Himedia). Human umbilical vein endothelial cells (HUVEC) (purchased from Lonza) were cultured in endothelial cell growth media (EGM, Lonza) containing heat-inactivated 2% fetal bovine serum (FBS), human VEGF, epidermal growth factor (EGF), insulin-like growth factor-1 (IGF-1), basic fibroblast growth factor (FGFB) and amphotericin-B. All cells were maintained at 37 °C incubator with 5% CO_2 in a humid atmosphere. Cells were allowed to grow for 60 h. In each case, cells were splited with trypsin-EDTA (Himedia, Bangalore) and 20 thousand cells present in 1 ml were seeded on the glass cover slips coated with or without hydrogel and allowed to grow for 24 h. Cells were fixed gently by adding 4% PFA directly into the cell culture media. The cells were subsequently permeabilized with 0.1% Triton-X100 (Sigma) and stained by DAPI (5 μM) to visualize the nucleus. Actin cytoskeleton was stained as described before (Goswami & Hucho, 2007). Alexa-488-labeled phalloidin (1:200) or Alexa-594-labeled phalloidin (1:200) was used to visualize polymerized actin cytoskeleton.

2.6. Live cell imaging

Approximately 3 micro liter of hydrogel was spotted on 22 mm glass cover slips and were air dried and placed on the custom made metal chamber suitable for live cell imaging. Approximately 10,000 freshly passage RAW264.7 cells were taken in 1 ml of media and were subject to labeling with dihexyloxacarbo-cyanine iodide dye (2 μM, MP, Biomedicals). After that the cell suspension was added on the glass cover slip and continuous image was taken for total 1 h with an interval of 1 min. The cells were imaged by using a confocal microscope (Zeiss, LSM780) using the 63× objective. All images were taken by same conditions for comparative analysis. Cells were exited by wavelength set at 490–543 (by using Argon laser, 1.8% power). Images were analyzed and processed by using LSM Image Examiner software.

3. Results

For the synthesis of hydrogels, the reaction was carried out by using different mole ratios of CMT and HEMA in the presence of benzoyl peroxide as initiator. In order to observe the changes in the appearance of the hydrogels, images of the final products were considered (Supplementary Figure 1). The optical properties indicate the relative changes in grafting as the respective color of the hydrogels range from near-white translucent to creamy white color as the CMT and HEMA ratio changes from 1:0.5 to 1:10. As the ratio changes further, the respective colors became darker again (from ratio 1:20 to 1:50). At a ratio of 1:50, the two components reveal two different layers indicating a phase separation. We attribute this trend in color to the increment in grafting with increased mole ratio for HEMA. This increment reaches its maxima when CMT:HEMA mole ratio became 1:10. Further increment in the HEMA ratio results in less grafting and also results in phase separation (when CMT and HEMA was used at 1:30 as well as 1:50 mole ratios). As these hydrogels were not grafted properly, these materials with less grafting properties were not characterized further.

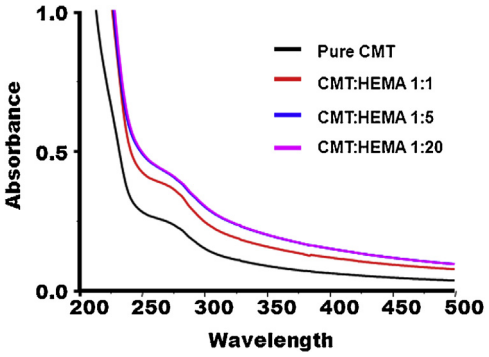

Fig. 1. UV spectra of hydrogels with different mole ratio of CMT to HEMA.

Supplementary data associated with this article can be found, in the online version, at http://dx.doi.org/10.1016/j.carbpol.2013.10.047.

Further these materials were characterized by UV visible spectra and FTIR spectra. For taking UV spectra, 0.05% (w/v) solution was prepared with distilled water. The absorbance is increased for hydrogels with increasing HEMA to CMT composition with respect to pure CMT. This increase in absorbance indicates about the increasing percentage of grafting of HEMA to the CMT (Fig. 1). Acquiring UV spectra for 1:10 ratio of CMT: HEMA was not possible as at this ratio it formed suspension in water. Subsequently, the samples were analyzed by FTIR and spectra were collected at the range 500–4000 cm^{-1} (Fig. 2). All the hydrogels of different mole ratio of CMT:HEMA have characteristic broad peak for hydroxyl group at 3600 cm^{-1}. The bands at 2925 and 2850 cm^{-1} are due to asymmetric and symmetric C—H stretching vibrations (Sen & Pal, 2009). The peak at 1132 cm^{-1} is due to C—O stretching. Further, the peak around 1620 and 1414 cm^{-1} corresponds to asymmetric and symmetric stretches of COO^- for pure CMT (Sen & Pal, 2009). There is a shift in asymmetric stretching peak to 1565 cm^{-1} for COO^- after grafting takes place for different hydrogels. However the intense peak at 1620 cm^{-1} reappears for 1:20 mole ratio of CMT:HEMA which can be attributed to the decrease in grafting percentage. The shift of CO peak from normal carbonyl (1735 cm^{-1}) peak to around 1570 cm^{-1} corresponds to a change in bond arrangement into one and half bond linkages in carboxylate (COO^-) (Ibrahim, Nada, & Kmal, 2005).

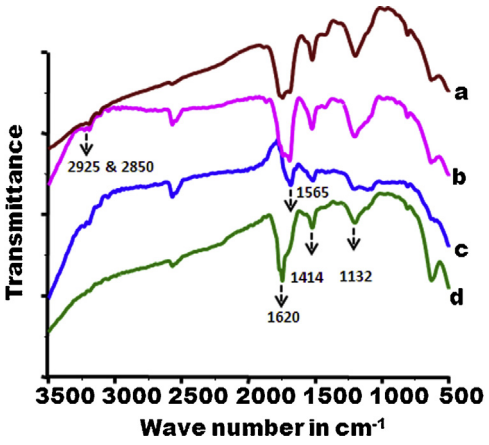

Fig. 2. FTIR spectra of hydrogels of different CMT:HEMA compositions. (a) CMT:HEMA (1:20), (b) CMT:HEMA (1:10), (c) CMT:HEMA (1:20), (d) pure CMT.

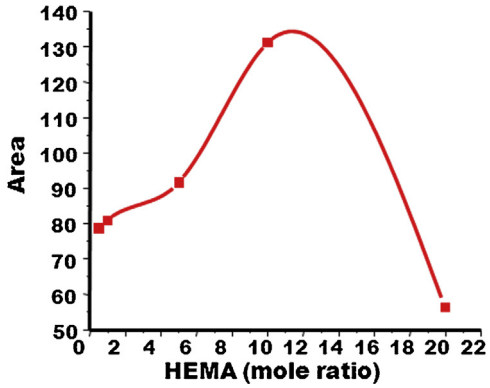

Fig. 3. The grafting profile as calculated from FTIR for hydrogels with increasing HEMA mole ratio to CMT.

Next we tested the extent of grafting by using FT-IR spectroscopy (Fig. 3). These results also reveal increased grafting properties with the increment in HEMA mole ratio with respect to CMT. In accordance with the optical properties, the IR spectroscopic analysis also indicate that the highest grafting occurs for CMT:HEMA at a mole ratio of 1:10, beyond which it declines again. The IR spectroscopic analysis elucidates insertion of HEMA on CMT backbone. The grafting yield was calculated from IR analysis followed by the gravimetric trend (data not shown). These results also reflect that CMT and HEMA produce the best grafted product at a mole ratio of 1:10 (Fig. 3).

In order to characterize these materials further, we performed swelling study. Hydro-swelling kinetics reflects relative increment in hydrophobic character of hydrogels. The swelling study depicts that there is decrease in quantity of water present as the HEMA content increases in the hydrogels (Fig. 4). This suggests that the hydrophobic character of hydrogel is increasing with HEMA content. However, the increment in hydrophobicity reaches its maxima with 1:10 ratio of CMT:HEMA composition and then decreases as shown in the case of 1:20 composition (Fig. 4).

Next we tested the CMT:HEMA (1:10) hydrogel for its biocompatibility. For that purpose we coated the hydrogel sample as a small spots on the glass cover slips and tested for cell growth on these surfaces, especially on the hydrogels. We used different cell lines, namely Neuro2a and RAW264.7 cell line which represent neuronal and osteoclast-precursor cells respectively (Dalbeth et al., 2008; Hase, Kanno, Kojima, Sakurai, & Kobata, 2008; Islam et al., 2007; Pederson, Ruan, Westendorf, Khosla, & Oursler, 2008; Vaananen, Zhao, Mulari, & Halleen, 2000). We noted that Neuro2a cells grow normally on this hydrogel (data not shown). Neuro2a cells growing directly on the hydrogel do not differ in their morphology from the Neuro2a cells that are growing on the glass surface. Therefore the effect of CMT:HEMA hydrogel on the Neuro2a cells mostly remain neutral and it exerts neither any positive effect nor any deleterious effect on Neuro2a cells as observed by morphological analysis. No specific dense growth of the Neuro2a cells was observed when allowed to grow on the hydrogels. In this case, Neuro2a cells grow uniformly all over the cover slips (data not shown).

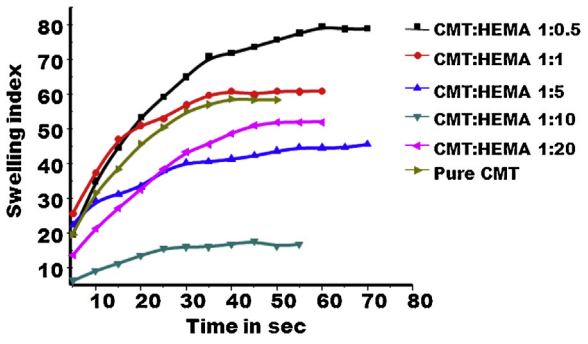

Fig. 4. Swelling kinetics of hydrogels with different mole ratios of CMT to HEMA.

Next we tested the effect of CMT:HEMA hydrogel on the RAW264.7 cell line. We noted that number of RAW264.7 cells growing on the hydrogel is much more when compared with the number of cells that are growing on the glass surface only (Fig. 5a). The pattern of growth behavior of RAW264.7 cells on the hydrogel is different when compared to Neuro2a cells. This uneven distribution with maximum cellular density on the hydrogel coated area indicates a specific and positive effect of CMT:HEMA (1:10) hydrogel on the adhesion of RAW264.7 cells. For that purpose we analyzed the distribution of actin cytoskeleton by staining the cells with Alexa-488 labeled phalloidin. We also analyzed the focal adhesion points at the hydrogel surface. We observed presence of multiple well defined focal adhesion points at the bottom surface of the cells which are growing on the hydrogels and suggests for a more adherent nature of the RAW264.7 cells on this surface (Fig. 5b and c). The dense growth of cells was observed for a long duration, i.e. even after 4th day of plating, indicating that this hydrogel is fully compatible with this cell for prolonged culture (data not shown).

As RAW264.7 cells reveals crowded growth specifically on the hydrogel surface 24 h after plating, we explored if this cells directly adhere on the hydrogel specifically at the early time points or migrate later on due to any chemo attractant activity exerted by CMT:HEMA (1:10) hydrogel. For that purpose, we labeled RAW264.7 cells with a fluorescent dye and performed live cell imaging to explore the cell adhesion properties (Fig. 6). For that purpose we visualized cell adhesion on the hydrogel surface as well as on glass cover slips. The faint green autofluorescence property of the dried hydrogel allowed us to demarcate the exact border of the CMT:HEMA (1:10) hydrogel spot on the glass cover slip. On plating a RAW264.7 cell suspension on the cover slips, we noted that more number of cells specifically adhere on the hydrogel surface and remain attached throughout the imaging time. Even cells attach on the hydrogel surface earlier than on the glass cover slips. This confirms that RAW264.7 cells prefers to adhere directly on CMT:HEMA (1:10) hydrogel.

Next we explored the compatibility of this surface for potential application in human. For that purpose we used a very sensitive primary cells from human origin, namely human umbilical vein endothelial cells (HUVEC) and tested if HUVEC cells can grow on the CMT:HEMA (1:10) surface. We observed that the endothelial cells grow normally on this surface (Fig. 7). No difference was observed in the cellular morphology in the HUVEC grown on glass coverlips or on CMT:HEMA (1:10) surface. This confirms that that surface bears no cytotoxicity for future application in human cells.

4. Discussion

Biomaterials are developed in order to evaluate, treat, augment or replace human tissue, organ or function. In this context, biocompatibility is the main prerequisite for their safe use as medical devices. Hydogels made of natural biopolymers offers materials for tissue engineering with ample biocompatibility. Hydrogels are three-dimensional networks capable of imbibing large amounts of water or biological fluids without affecting its three-dimensional network structure, a property which resemble them large extent to the biological tissues (Karlsson & Gatenholm, 1997; Pal, Banthia, & Majumdar, 2009; Peppas, Bures, Leobandung, & Ichikawa, 2000). In particular, the water imbibing capacity and rubbery nature of hydrogels resembles to the natural tissues. The hydrogels

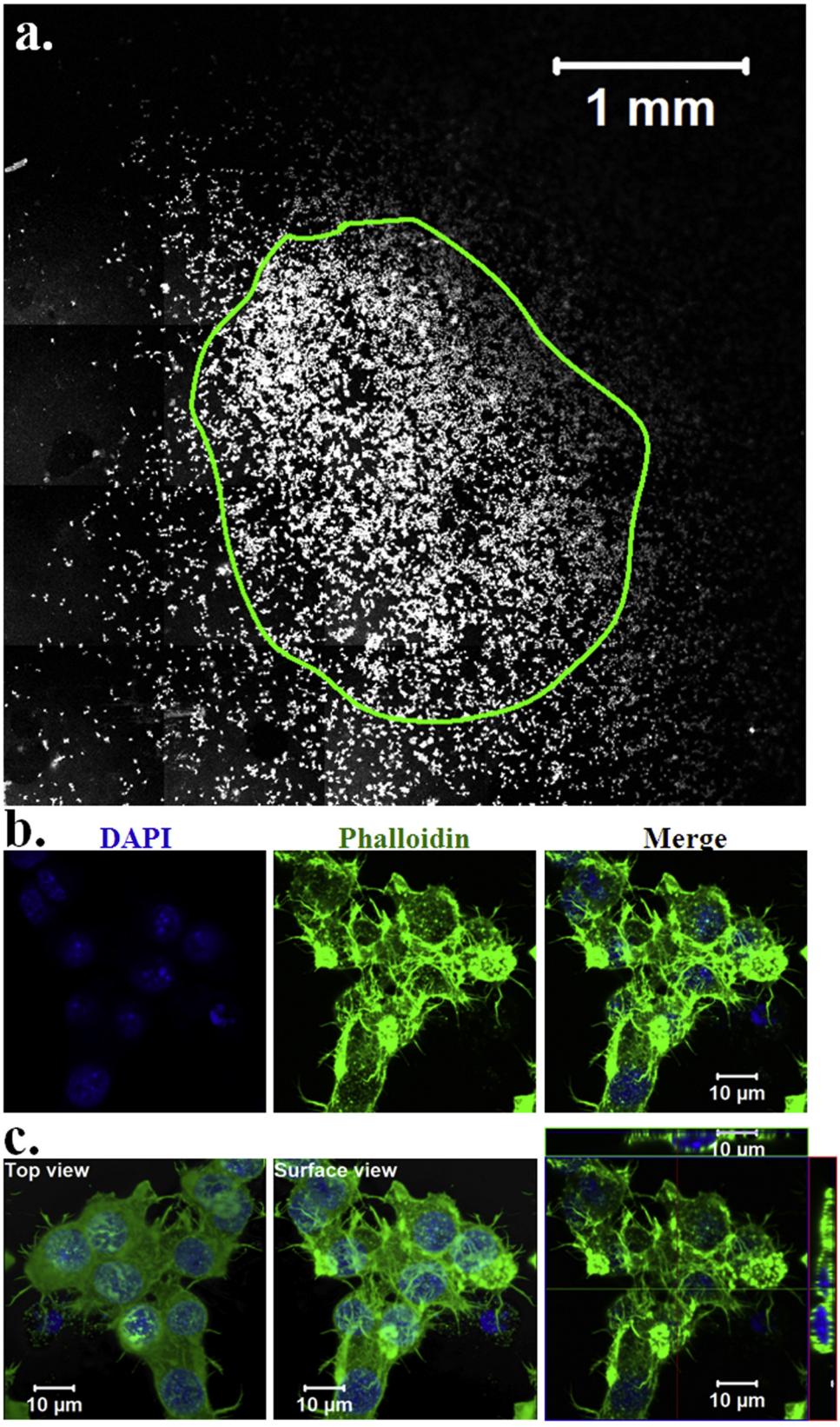

Fig. 5. CMT:HEMA (1:10) hydrogel is biocompatible for bone precursor cells. (a) Cells were grown on hydrogels (borders of such hydrogel spot is indicated by green line), fixed and the nucleus of the attached cells were stained with DAPI. Cells effectively grow on the hydrogel surface. (b) Shown are the confocal images of cells grown on CMT:HEMA surface. Cells were grown for 24 h on this surface before fixing. Cells were stained for polymerized F-actin fiber by Alexa-488 labeled phalloidin (green) and DNA by DAPI (blue). (c) Enlarged 3D merged images of the culture are shown. The top view (left), bottom surface view (middle) and ortho-representation (right) indicate the filopodial structures, focal adhesion points and the surface attachments in details. (For interpretation of the references to color in this figure legend, the reader is referred to the web version of the article.)

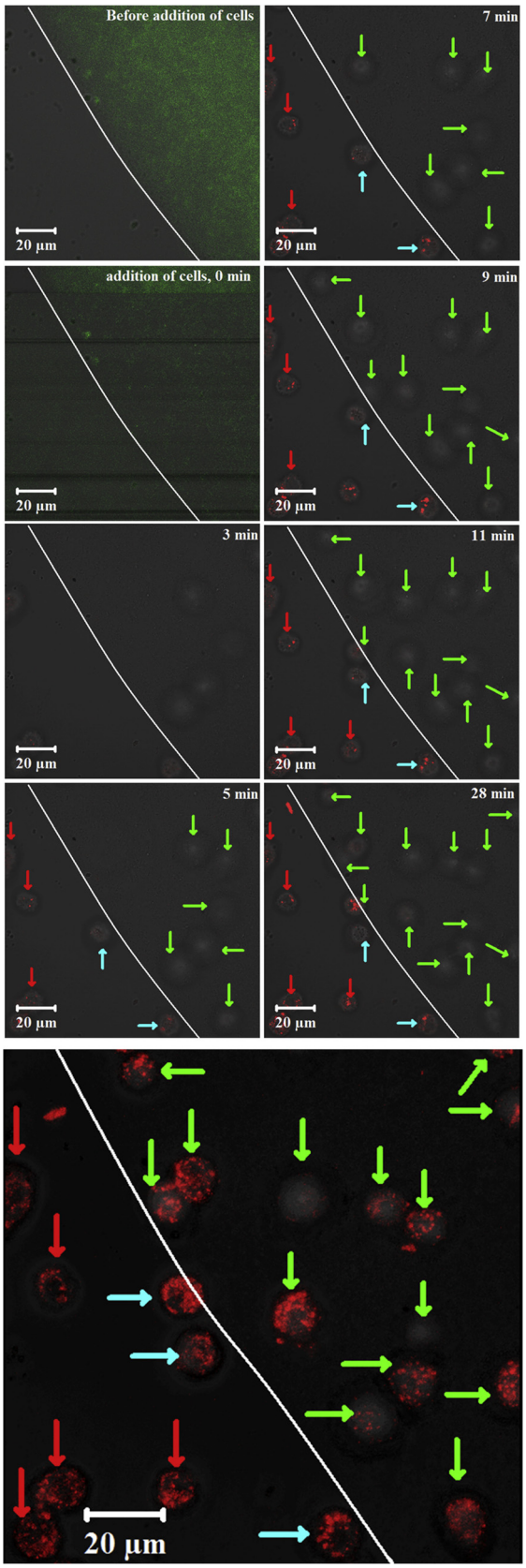

Fig. 6. Specific adhesion of cells on the hydrogel surface. Shown are the life cell experiments demonstrating the adhesion of cells on the hydrogel surface (indicated by the white border line). Cells were stained with a fluorescently active dye and the cell suspension was added to the hydrogel surface for settling of cells. Green, blue and red arrows indicate the cells that adhere directly to the hydrogel surface, to the hydrogel border and to the glass surface respectively. The relative morphology and the nature of the cells at the end of experiments are shown in below. (For interpretation of the references to color in this figure legend, the reader is referred to the web version of the article.)

synthesized from polysaccharides such as from natural gums have good biocompatibility and biological inertness. Because of these characteristics, hydrogels have been extensively used in the biomedical and pharmaceutical industries such as for making contact lenses, biosensors, membranes, artificial organs, and carriers for controlled drug delivery (Peppas et al., 2000). The high water content also leads to low mechanical strength which in some cases limits specific applications. The hydrogels are insoluble due to the presence of chemical cross-links (tie-points, junctions) and/or physical cross-links (such as entanglements and crystallites) (Karlsson & Gatenholm, 1997; Peppas et al., 2000). These materials can be synthesized to respond to a number of physiological stimuli present in the body, such as pH, ionic strength and temperature (Pal et al., 2009; Peppas et al., 2000; Qiu & Park, 2001). The mechanical performance of hydrogels can be improved by increasing the crosslink density, forming interpenetrated networks or inducing crystallization (Bhattacharya & Misra, 2004; Karlsson & Gatenholm, 1997; Peppas et al., 2000). The most commonly used monomers for synthesis of hydrogels are mono- and multifunctional (meth) acrylates and their derivatives (Li & Lee, 2005). Several co-monomers are added to adjust the cross-linking density, thus modifying the swelling and mechanical properties of hydrogels (Karlsson & Gatenholm, 1997). For instance, diethylene glycol, dimethacylate (DEGDMA) are usually mixed with 2-hydroxyethyl methacrylate (HEMA) for preparing poly (HEMA) hydrogels (Hacioglu, Berchtold, Lovell, Nie, & Bowman, 2002; Li & Lee, 2005).

In this work we have taken carboxy methyl tamarind (CMT), a substituted polysaccharide prepared from tamarind kernel powder as a polysaccharide material (Goyal, Kumar, & Sharma, 2007; Sen & Pal, 2009). Polysaccharides are generally water soluble (Rana et al., 2011). Polysaccharide materials with extreme water solubility and/or susceptibility to degrading enzymes make them less suitable to be used as solid scaffolds/matrix. Therefore, proper hydrophilic–hydrophobic balance of a hydrogel is an important criterion suitable for their biological applications. In case of CMT, the —OH moieties are not able to form strong ionic interactions with counter ions (Hoare & Kohane, 2008; Rana et al., 2011). This limit CMT for effective biological applications and further custom-made improvement of CMT-based hydrogels are needed for specific applications.

Based on the FTIR spectral analysis, a probable mechanism can be proposed (Fig. 8). Previously Sen and Pal have showed that grafting of acrylamide on to CMT backbone takes place through O-atom (Sen & Pal, 2009). Here we suggest a similar microarchitecture in the CMT–HEMA-based hydrogel/s. The IR peak at 1120 cm^{-1} in grafted hydrogel indicates that the grafting has taken place through the O-atom forming C—O—C linkage. The intensity of this peak increases with increment in grafting percentage corresponding to the increase in HEMA content. The absence of carbonyl peak around 1700 cm^{-1} suggests most probably the co-polymerization has taken place without ring opening during or after grafting of 2-HEMA onto the CMT backbone. The prominence of peak intensity at 2925 cm^{-1} may be attributed to the increase in grafted polymerized HEMA.

In order to convert CMT suitable for biological applications, potentially different functional groups can be introduced (Rana et al., 2011). Previously it was observed that different groups such as carboxyl groups, carboxymethyl groups, polyacrylamide groups, phosphate groups etc. increases its hydrophobicity (Rana et al., 2011). Notably, altering the functionality depends on cross-linking density, i.e. the mole ratio of cross-linking agent to the moles of

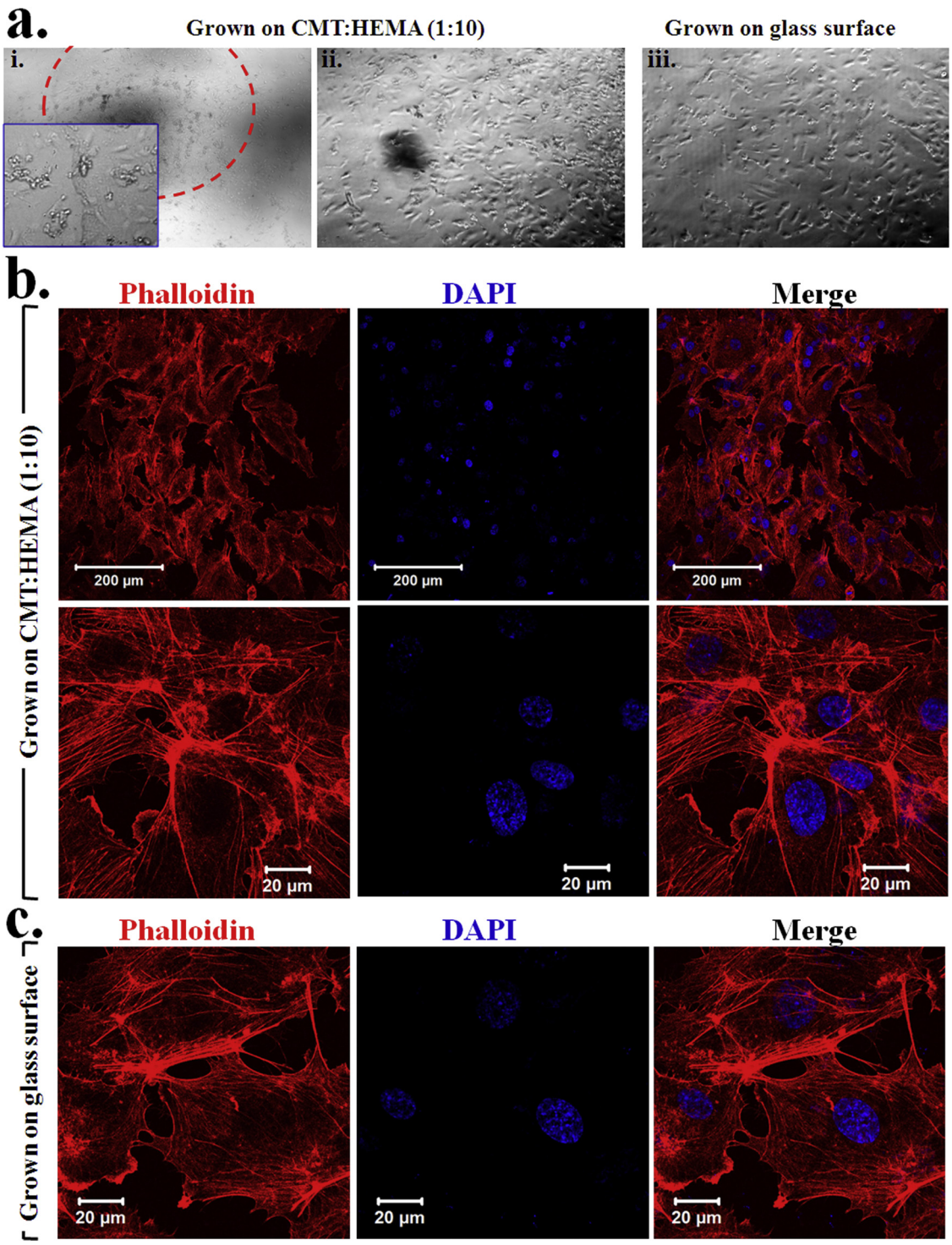

Fig. 7. Biocompatibility of human umbilical vein endothelial cells on CMT:HEMA (1:10) surface. (a) Shown are the phase contrast images of HUVEC cells grown for 60 h on CMT:HEMA surface (i–ii) in lower magnification (i) and higher magnification (ii). Similarly cells grown on glass surface are also shown (iii). The border of the hydrogel surface with cells is shown in set (i). (b) Shown are the confocal images of HUVEC cells grown on CMT:HEMA surface. Cells were grown for 60 h of on this surface before fixing. Cells were stained for polymerized F-actin fiber by Alexa-594 labeled phalloidin (red) and DNA by DAPI (blue). An enlarged view of the culture is shown in the lower panel. (c) Confocal images of HUVEC cells grown on glass surface are shown. No differences were observed when HUVEC cells were grown on glass surface or on CMT:HEMA (1:10) surface. (For interpretation of the references to color in this figure legend, the reader is referred to the web version of the article.)

polymer repeating units (Rana et al., 2011). Moreover cross-linking density is critical for the desirable polymeric net formation and its application for desired purpose (Lee & Mooney, 2001; Rana et al., 2011). However, in this work we have modified CMT by another material, namely by 2-Hydroxyethyl methacrylate (HEMA). HEMA is a hydrophilic, surface-active compound, has dual functionality monomer and also available in highly pure form. Owing to these advantages we have used HEMA along with CMT to prepare a novel hydrogel. So far HEMA has been widely used in its polymeric form in numerous biomedical applications (Sun, Huang, Lin, & Lai, 1997). HEMA can be polymerized either by homopolymerization or copolymerization technique (Mabilleau, Moreau, Filmon,

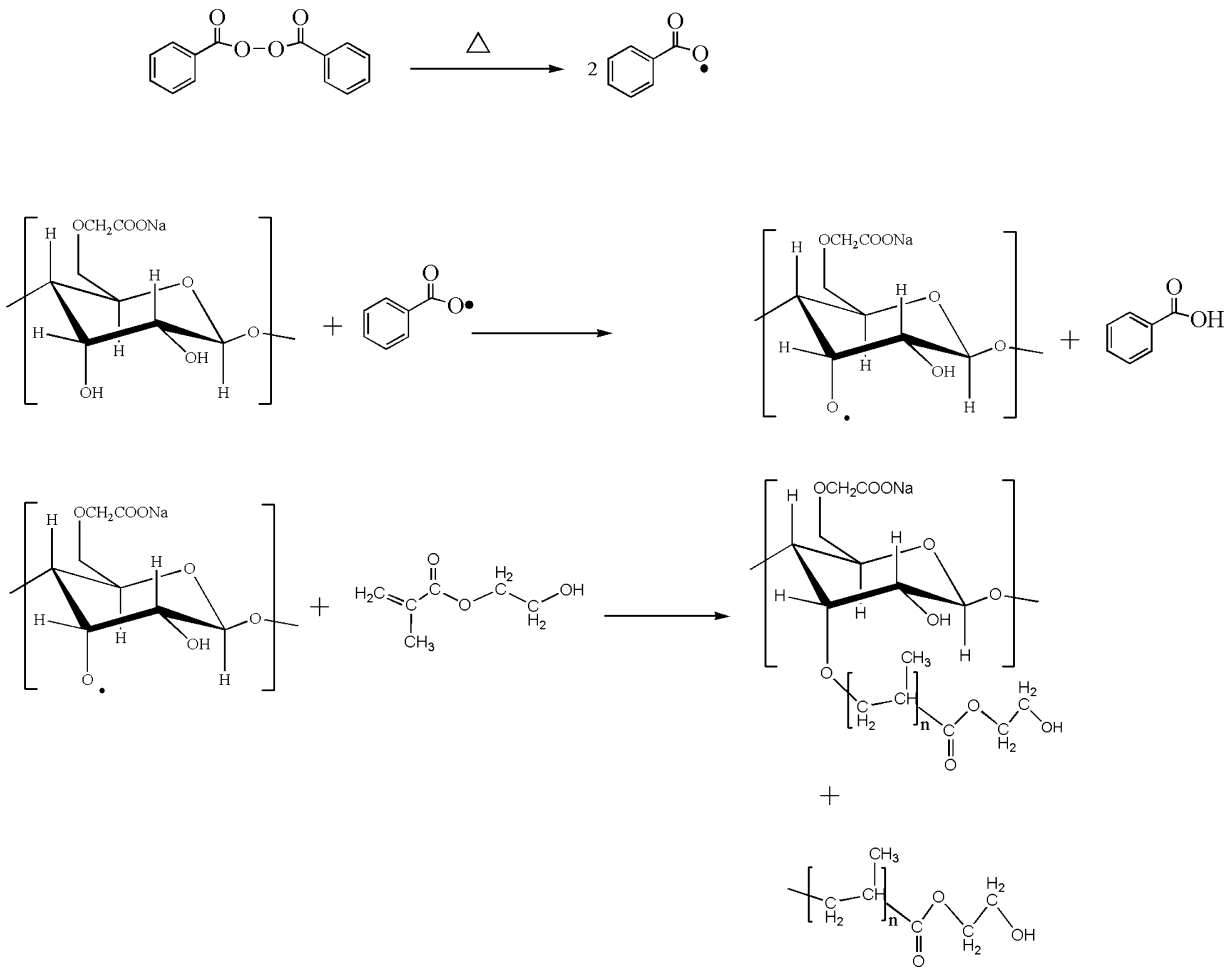

Fig. 8. Probable mechanism of HEMA grafting on CMT polysachharide.

Baslé, & Chappard, 2004; Vazquez, Gurruchaga, & Goni, 1995). So far both homopolymeric and copolymeric forms of HEMA have been largely used in various applications (Chouhan & Bajpai, 2010). Due to biocompatibility; Poly (HEMA) can act as an ideal component for many biomedical and pharmaceutical applications, including optical lenses, implants, drug delivery devices, and support for enzyme immobilization (Mabilleau et al., 2004). Our work demonstrates that grafted CMT–HEMA at a ratio of 1:10 can be a good material for adhering and further growth of bone precursor cells suitable for bone tissue engineering.

The bone defects observed in patients in case of several diseases and pathophysiological conditions poses a serious clinical problem as well as economic and social burden to the population (Dimai et al., 2012; Tarride et al., 2012). The bone defects are common in old ages and in several pathophysiological situations such as accidents, cancer, osteoporosis and other bone-related problems where bone tissue engineering is a realistic hope (Girones Molera, Mendez, & San Roman, 2012; Mehta, Schmidt-Bleek, Duda, & Mooney, 2012; Rohrbach & Giunta, 2012). During tissue morphogenesis and homeostasis, cells experience various signals in their environments, including gradients of physical and chemical cues. Spatial and temporal gradients regulate various cell behaviors such as proliferation, migration, differentiation during development, inflammation, wound healing, and cancer. Creation of microenvironments in the engineered three-dimensional (3D) scaffolds mimicking the in vivo cellular and tissue complexity by incorporating physical, chemical, spatio-temporal gradients and other parameters within engineered three-dimensional (3D) scaffolds is a fundamental aim relevant in tissue engineering. In that context, chemically modified hydrogels can act as ideal 3D tissue scaffolds by mimicking extracellular matrix (ECM) for specific cells (Sant, Hancock, Donnelly, Iyer, & Khademhosseini, 2010). Indeed, so far a large number of hydrogel products made of synthetic or natural polymers have been successfully used for clinical purpose. For example, soft contact lenses made from poly(hydroxyethylmethacrylic) acid [poly(HEMA)], surgical grade biological adhesives made from reconstituted fibrin or albumin, wound dressings made from alginate polysaccharide, fillers made from hyaluronic acid (HA) (Seliktar, 2012) have long history for successful clinical applications.

In this work we demonstrate that different sensitive cells such as bone precursor cells, neuronal cells and human umbilical vein endothelial cells (HUVEC) can grow successfully on this hydrogel surface. However, the growth pattern is largely different for different cell types ranging excellent growth to moderate growth for some cells. These also indicate that the surface and material properties are optimum for other cells and ideal if not excellent for preosteoclast (RAW264.7) cells and also for the HUVEC cells. The bone cells have been reported to be extremely sensitive in terms of their surface requirements as cell adhesion-mediated signaling events play a major role in the survival and chemotaxis events (Lee, Ko, & Kim, 2006). Non-compatible surfaces can induce apoptosis in osteoblasts and cause major bone defects (Grigoriou et al., 2005). Preosteoclast cells studied in this work can proliferate easily on this surface for a long duration without any symptom of cytotoxicity and form dense clusters (till 100 h as observed in

this study) indicating that this surface offers positive adhesion and focal signaling events relevant for preosteoclast cell adhesion and further growth. The fast adhesion and further growth as well as clustering of preosteoclast cells on this surface are most likely due to the compatible properties of the cell adhesion molecules, specific receptors, ion channels and intrinsic affinity of this cells for complex carbohydrate molecules. In agreement with this, we demonstrate that the preosteoclast cells adhere well on this surface and their filopodial structures are well spread. The focal adhesion points are distinct. This observation is in accordance with several reports suggesting that integrin- and focal adhesion-mediated signaling events play key roles in bone cell adhesion, chemotaxis, growth, differentiation and maturation (Carvalho, Kostenuik, Salih, Bumann, & Gerstenfeld, 2003; Cheng, Lai, Blystone, & Avioli, 2001; Damsky, 1999; Kim et al., 2007; Nakayamada, Okada, Saito, Tamura, & Tanaka, 2003; Salasznyk, Klees, Williams, Boskey, & Plopper, 2007). The early events of cell adhesion and further growth also suggest that this surface is better than few other surfaces prepared before where cell adhesion is either poor and takes long time or the surface exerts cytotoxicity (Lai et al., 2010).

5. Conclusion

All the characterization result suggests that CMT:HEMA in 1:10 mole ratio provides the best grafted hydrogel. We conclude that this novel hydrogel made of CMT:HEMA has a potentiality for its application in bone-tissue engineering. Successful attachment and growth of HUVEC cells on this surface also suggest that this surface can also be used in human and can be used to induce cell and tissue differentiation. However, further human bone cell specific studies are required in future.

Acknowledgement

The authors acknowledge Hindustan Gums Pvt. Limited for providing Carboxy methyl Polysaccharide powder.

References

Azami, M., Tavakol, S., Samadikuchaksaraei, A., Hashjin, M. S., Baheiraei, N., Kamali, M., et al. (2012). A porous hydroxyapatite/gelatin nanocomposite scaffold for bone tissue repair: In vitro and in vivo evaluation. *Journal of Biomaterials Science Polymer Edition*, *23*, 2353–2368.

Bhattacharya, A., & Misra, B. N. (2004). Grafting: A versatile means to modify polymers: Techniques, factors and applications. *Progress in Polymer Science*, *29*, 767–814.

Carvalho, R. S., Kostenuik, P. J., Salih, E., Bumann, A., & Gerstenfeld, L. C. (2003). Selective adhesion of osteoblastic cells to different integrin ligands induces osteopontin gene expression. *Matrix Biology*, *22*, 241–249.

Cheng, S. L., Lai, C. F., Blystone, S. D., & Avioli, L. V. (2001). Bone mineralization and osteoblast differentiation are negatively modulated by integrin alpha(v)beta3. *Journal of Bone and Mineral Research*, *16*, 277–288.

Chouhan, R., & Bajpai, A. K. (2010). Release dynamics of ciprofloxacin from swellable nanocarriers of poly(2-hydroxyethyl methacrylate): An in vitro study. *Nanomedicine*, *6*, 453–462.

Dalbeth, N., Smith, T., Nicolson, B., Clark, B., Callon, K., Naot, D., et al. (2008). Enhanced osteoclastogenesis in patients with tophaceous gout: Urate crystals promote osteoclast development through interactions with stromal cells. *Arthritis and Rheumatism*, *58*, 1854–1865.

Damsky, C. H. (1999). Extracellular matrix–integrin interactions in osteoblast function and tissue remodeling. *Bone*, *25*, 95–96.

Dimai, H. P., Redlich, K., Peretz, M., Borgstrom, F., Siebert, U., & Mahlich, J. (2012). Economic burden of osteoporotic fractures in Austria. *Health Economics Review*, *2*, 12.

Giannoudis, P. V., Dinopoulos, H., & Tsiridis, E. (2005). Bone substitutes: An update. *Injury*, *36*(Suppl. 3), S20–S27.

Girones Molera, J., Mendez, J. A., & San Roman, J. (2012). Bioresorbable and nonresorbable polymers for bone tissue engineering. *Current Pharmaceutical Design*, *18*, 2536–2557.

Glaesemann, B. P. (2011). *Ovalbumin-based scaffolds reinforced with cellulose nanocrystals for bone tissue engineering*. Virginia: Blacksburg (Thesis)

Goswami, C., & Hucho, T. (2007). TRPV1 expression-dependent initiation and regulation of filopodia. *Journal of Neurochemistry*, *103*, 1319–1333.

Goyal, P., Kumar, V., & Sharma, P. (2007). Carboxymethylation of Tamarind kernel powder. *Carbohydrate Polymers*, *69*, 251–255.

Grigoriou, V., Shapiro, I. M., Cavalcanti-Adam, E. A., Composto, R. J., Ducheyne, P., & Adams, C. S. (2005). Apoptosis and survival of osteoblast-like cells are regulated by surface attachment. *Journal of Biological Chemistry*, *280*, 1733–1739.

Hacioglu, B., Berchtold, K. A., Lovell, L. G., Nie, J., & Bowman, C. N. (2002). Polymerization kinetics of HEMA/DEGDMA: Using changes in initiation and chain transfer rates to explore the effects of chain-length-dependent termination. *Biomaterials*, *23*, 4057–4064.

Hase, H., Kanno, Y., Kojima, H., Sakurai, D., & Kobata, T. (2008). Coculture of osteoclast precursors with rheumatoid synovial fibroblasts induces osteoclastogenesis via transforming growth factor beta-mediated down-regulation of osteoprotegerin. *Arthritis and Rheumatism*, *58*, 3356–3365.

Hefti, T., Frischherz, M., Spencer, N. D., Hall, H., & Schlottig, F. (2010). A comparison of osteoclast resorption pits on bone with titanium and zirconia surfaces. *Biomaterials*, *31*, 7321–7331.

Hoare, T. R., & Kohane, D. S. (2008). Hydrogels in drug delivery: Progress and challenges. *Polymer*, *49*, 1993–2007.

Ibrahim, M., Nada, A., & Kamal, D. E. (2005). Density functional theory and FTIR spectroscopic study of carboxyl group. *Indian Journal of Pure & Applied Physics*, *43*, 911–917.

Islam, S., Hassan, F., Tumurkhuu, G., Dagvadorj, J., Koide, N., Naiki, Y., et al. (2007). Bacterial lipopolysaccharide induces osteoclast formation in RAW 264.7 macrophage cells. *Biochemical and Biophysical Research Communications*, *360*, 346–351.

Karlsson, J. O., & Gatenholm, P. (1997). Preparation and characterization of cellulose-supported HEMA hydrogels. *Polymer*, *38*, 4727–4731.

Khatiwala, C. B., Peyton, S. R., & Putnam, A. J. (2006). Intrinsic mechanical properties of the extracellular matrix affect the behavior of pre-osteoblastic MC3T3-E1 cells. *American Journal of Physiology – Cell Physiology*, *290*, C1640–C1650.

Kim, J. B., Leucht, P., Luppen, C. A., Park, Y. J., Beggs, H. E., Damsky, C. H., et al. (2007). Reconciling the roles of FAK in osteoblast differentiation, osteoclast remodeling and bone regeneration. *Bone*, *41*, 39–51.

Krause, A., Cowles, E. A., & Gronowicz, G. (2000). Integrin-mediated signaling in osteoblasts on titanium implant materials. *Journal of Biomedical Materials Research*, *52*, 738–747.

Lai, H. C., Zhuang, L. F., Liu, X., Wieland, M., Zhang, Z. Y., & Zhang, Z. Y. (2010). The influence of surface energy on early adherent events of osteoblast on titanium substrates. *Journal of Biomedical Materials Research Part A*, *93*, 289–296.

Langer, R., & Vacanti, J. P. (1993). Tissue engineering. *Science*, *260*(5110), 920–926.

Lee, K. Y., & Mooney, D. J. (2001). Hydrogels for tissue engineering. *Chemical Reviews*, *101*, 1869–1879.

Lee, Y. J., Ko, J. S., & Kim, H. M. (2006). The role of cell signaling defects on the proliferation of osteoblasts on the calcium phosphate apatite thin film. *Biomaterials*, *27*, 3738–3744.

Li, L., & Lee, L. J. (2005). Photopolymerization of HEMA/DEGDMA hydrogels in solution. *Polymer*, *46*, 11540–11547.

Lieb, E., Tessmar, J., Hacker, M., Fischbach, C., Rose, D., Blunk, T., et al. (2003). Poly(D,L-lactic acid)-poly(ethylene glycol)-monomethyl ether diblock copolymers control adhesion and osteoblastic differentiation of marrow stromal cells. *Tissue Engineering*, *9*, 71–84.

Malheiro, V. N., Spear, R. L., Brooks, R. A., & Markaki, A. E. (2011). Osteoblast and monocyte responses to 444 ferritic stainless steel intended for a magneto-mechanically actuated fibrous scaffold. *Biomaterials*, *32*, 6883–6892.

Mabilleau, G., Moreau, M. F., Filmon, R., Basle, M. F., & Chappard, D. (2004). Biodegradability of poly (2-hydroxyethyl methacrylate) in the presence of the J774.2 macrophage cell line. *Biomaterials*, *25*, 5155–5162.

Mehta, M., Schmidt-Bleek, K., Duda, G. N., & Mooney, D. J. (2012). Biomaterial delivery of morphogens to mimic the natural healing cascade in bone. *Advanced Drug Delivery Reviews*, *64*, 1257–1276.

Nakayamada, S., Okada, Y., Saito, K., Tamura, M., & Tanaka, Y. (2003). Beta1 integrin/focal adhesion kinase-mediated signaling induces intercellular adhesion molecule 1 and receptor activator of nuclear factor kappaB ligand on osteoblasts and osteoclast maturation. *Journal of Biological Chemistry*, *278*, 45368–45374.

Nauth, A., McKee, M. D., Einhorn, T. A., Watson, J. T., Li, R., & Schemitsch, E. H. (2011). Managing bone defects. *Journal of Orthopaedic Trauma*, *25*, 462–466.

Pal, K., Banthia, A. K., & Majumdar, D. K. (2009). Polymeric hydrogels: Characterization and biomedical applications—A mini review. *Designed Monomers and Polymers*, *12*, 197–220.

Pederson, L., Ruan, M., Westendorf, J. J., Khosla, S., & Oursler, M. J. (2008). Regulation of bone formation by osteoclasts involves Wnt/BMP signaling and the chemokine sphingosine-1-phosphate. *Proceedings of the National Academy of Sciences of the United States of America*, *105*, 20764–20769.

Peppas, N. A., Bures, P., Leobandung, W., & Ichikawa, H. (2000). Hydrogels in pharmaceutical formulations. *European Journal of Pharmaceutics and Biopharmaceutics*, *50*, 27–46.

Qiu, Y., & Park, K. (2001). Environment-sensitive hydrogels for drug delivery. *Advanced Drug Delivery Reviews*, *53*, 321–339.

Rana, V., Rai, P., Tiwary, A. K., Singh, R. S., Kennedy, J. F., & Knill, C. J. (2011). Modified gums: Approaches and applications in drug delivery. *Carbohydrate Polymers*, *83*, 1031–1047.

Reikeras, O., Shegarfi, H., Naper, C., Reinholt, F. P., & Rolstad, B. (2008). Impact of MHC mismatch and freezing on bone graft incorporation: An experimental study in rats. *Journal of Orthopaedic Research*, *26*, 925–931.

Reikeras, O., Sigurdsen, U. W., & Shegarfi, H. (2010). Impact of freezing on immunology and incorporation of bone allograft. *Journal of Orthopaedic Research*, *28*, 1215–1219.

Rohrbach, M., & Giunta, C. (2012). Recessive osteogenesis imperfecta: Clinical, radiological, and molecular findings. *American Journal of Medical Genetics Part C Seminars in Medical Genetics*, *160C*, 175–189.

Salasznyk, R. M., Klees, R. F., Williams, W. A., Boskey, A., & Plopper, G. E. (2007). Focal adhesion kinase signaling pathways regulate the osteogenic differentiation of human mesenchymal stem cells. *Experimental Cell Research*, *313*, 22–37.

Sant, S., Hancock, M. J., Donnelly, J. P., Iyer, D., & Khademhosseini, A. (2010). Biomimetic gradient hydrogels for tissue engineering. *Canadian Journal of Chemical Engineering*, *88*, 899–911.

Seliktar, D. (2012). Designing cell-compatible hydrogels for biomedical applications. *Science*, *336*(6085), 1124–1128.

Sen, G., & Pal, S. (2009). Polyacrylamide grafted carboxymethyl tamarind (CMT-g-PAM): Development and application of a novel polymeric flocculant. *Macromolecular Symposium*, *277*, 100–111.

Shih, Y. R., Tseng, K. F., Lai, H. Y., Lin, C. H., & Lee, O. K. (2011). Matrix stiffness regulation of integrin-mediated mechanotransduction during osteogenic differentiation of human mesenchymal stem cells. *Journal of Bone and Mineral Research*, *26*, 730–738.

Shegarfi, H., & Reikeras, O. (2009). Review article: Bone transplantation and immune response. *Journal of Orthopaedic Surgery (Hong Kong)*, *17*, 206–211.

Slaughter, B. V., Khurshid, S. S., Fisher, O. Z., Khademhosseini, A., & Peppas, N. A. (2009). Hydrogels in regenerative medicine. *Advanced Materials*, *21*, 3307–3329.

Sun, Y. M., Huang, J. J., Lin, F. C., & Lai, J. Y. (1997). Composite poly(2-hydroxyethyl methacrylate) membranes as rate-controlling barriers for transdermal applications. *Biomaterials*, *18*, 527–533.

Tarride, J. E., Guo, N., Hopkins, R., Leslie, W. D., Morin, S., Adachi, J. D., et al. (2012). The burden of illness of osteoporosis in Canadian men. *Journal of Bone and Mineral Research*, *27*, 1830–1838.

Thein-Han, W. W., & Misra, R. D. (2009). Biomimetic chitosan-nanohydroxyapatite composite scaffolds for bone tissue engineering. *Acta Biomaterialia*, *5*, 1182–1197.

Vaananen, H. K., Zhao, H., Mulari, M., & Halleen, J. M. (2000). The cell biology of osteoclast function. *Journal of Cell Science*, *113*(Pt 3), 377–381.

Vazquez, B., Gurruchaga, M., & Goni, I. (1995). Hydrogels based on graft copolymerization of HEMA/BMA mixtures onto soluble gelatin: Swelling behaviour. *Polymer*, *36*, 2311–2314.

Venkatesan, J., Ryu, B., Sudha, P. N., & Kim, S. K. (2012). Preparation and characterization of chitosan-carbon nanotube scaffolds for bone tissue engineering. *International Journal of Biological Macromolecules*, *50*, 393–402.

Yang, L., Chinthapenta, V., Li, Q., Stout, D., Liang, A., Sheldon, B. W., et al. (2011). Understanding osteoblast responses to stiff nanotopographies through experiments and computational simulations. *Journal of Biomedical Materials Research Part A*, *97*, 375–382.

Zambuzzi, W. F., Ferreira, C. V., Granjeiro, J. M., & Aoyama, H. (2011). Biological behavior of pre-osteoblasts on natural hydroxyapatite: A study of signaling molecules from attachment to differentiation. *Journal of Biomedical Materials Research Part A*, *97*, 193–200.

Zhang, L., Rodriguez, J., Raez, J., Myles, A. J., Fenniri, H., & Webster, T. J. (2009). Biologically inspired rosette nanotubes and nanocrystalline hydroxyapatite hydrogel nanocomposites as improved bone substitutes. *Nanotechnology*, *20*, 175101.

Ziane, S., Schlaubitz, S., Miraux, S., Patwa, A., Lalande, C., Bilem, I., et al. (2011). A thermosensitive low molecular weight hydrogel as scaffold for tissue engineering. *European Cells & Materials*, *23*, 147–160.